Electronic Supplementary Material (ESI) for New Journal of Chemistry.
This journal is © The Royal Society of Chemistry and the Centre National de la Recherche Scientifique 2017

Supplementary Information

An environment-friendly route to graphene oxide by concentrated ozone with improved catalytic performance

Jin Zhang,[ab] Ye Zhang,*[a] Ligong Zhou,[a] Ying Yang[a] and Xuekuan Li[a]

New Journal of Chemistry

[a.] *Institute of Coal Chemistry, Chinese Academy of Sciences, Taiyuan 030001, PR China*

[b.] *University of Chinese Academy of Sciences, Beijing 100049, PR China*

[*] E-mail: yzhang@sxicc.ac.cn

Experimental Section

Chemicals and Materials. Graphite powder and Ammonium Nitrate (NH_4NO_3) were purchased from Shanghai Chemical Reagent Company. Ozone generator was supplied by Wuhan WeiMeng Technology Company. Distilled water was used in the process of aqueous solution preparations. Ultrapure water was exclusively used for ozone generator.

Preparation of Graphene Oxide. In the first step, graphite powder (5.0 g) and NH_4NO_3 (20.0 g) were mixed with water in a 300 mL crucible with cover, followed by continuously stirring at room temperature for 12 h. Then the water was slowly evaporated at 80 ℃ to obtain solid mixture. The solids were transferred into a muffle furnace to expand at 390 ℃ for 30 min to get expanded sample G-NH_4NO_3. In the second step, G-NH_4NO_3 was mixed with distilled water in a 500 mL Monshells bottle

and heated to 33 ℃. Highly concentrated ozone generated from the ozone generator continuously passed through the graphite/water mixture for 18 h under stirring condition. The obtained graphite oxide solution was sonicated and centrifugated for 30 min respectively to get graphene oxide (GO) solution. The GO solid samples were separated from aqueous solutions by process of freeze-drying. Unreacted ozone was transferred to oxygen in another washing bottle.

Characterization. SEM images were collected on a Hitachi S4800 field-emission SEM system. X-ray diffraction (XRD) was carried out on a D8 Advance X-ray powder diffractometer using Cu Kα radiation. X-ray photoelectron spectroscopy (XPS) was conducted with an ultrahigh vacuum on a Kratos AXIS ULTRA DLD spectrometer with Al Kα radiation and a multichannel detector, the binding energies were referenced to the C1s at 284.6 eV. Raman spectroscopy was examined on a Raman Microprobe (HR-800 Jobin-Yvon) with 532 nm Nd: YAG excitation source at room temperature. Fourier transform infrared (FT-IR) spectra were recorded on a NEXUS 470 spectrometer. Atomic force micrographs (AFM) were obtained using a CSPM 5500 in the tapping mode. The investigation of the structure was carried out by a Transmission electron microscopy (TEM) using JEM-2010. Water bath sonication was performed with a KQ-800DB (100-800W).

Catalytic tests. All the reactions were performed in a 100 mL Teflon-lined stainless steel autoclave. Typically, Benzyl alcohol (1 mmol, 108 mg), acetonitrile (60 mL), TEMPO (1 mmol, 155 mg) and 50 mg GO were added into the reactor and then stayed at 150 ℃ for a certain time under oxygen or nitrogen atmosphere with stirring

conditions. The reactants and products were analyzed by Gas chromatography (Shimadzu GC-2010) with a flame ionization detector using a DB-1 capillary column (60 m × 0.25 mm × 0.25 μm). The conversion of reactant was expressed in mol %, based on the total benzyl alcohol amount. The products were identified by GC-MS.

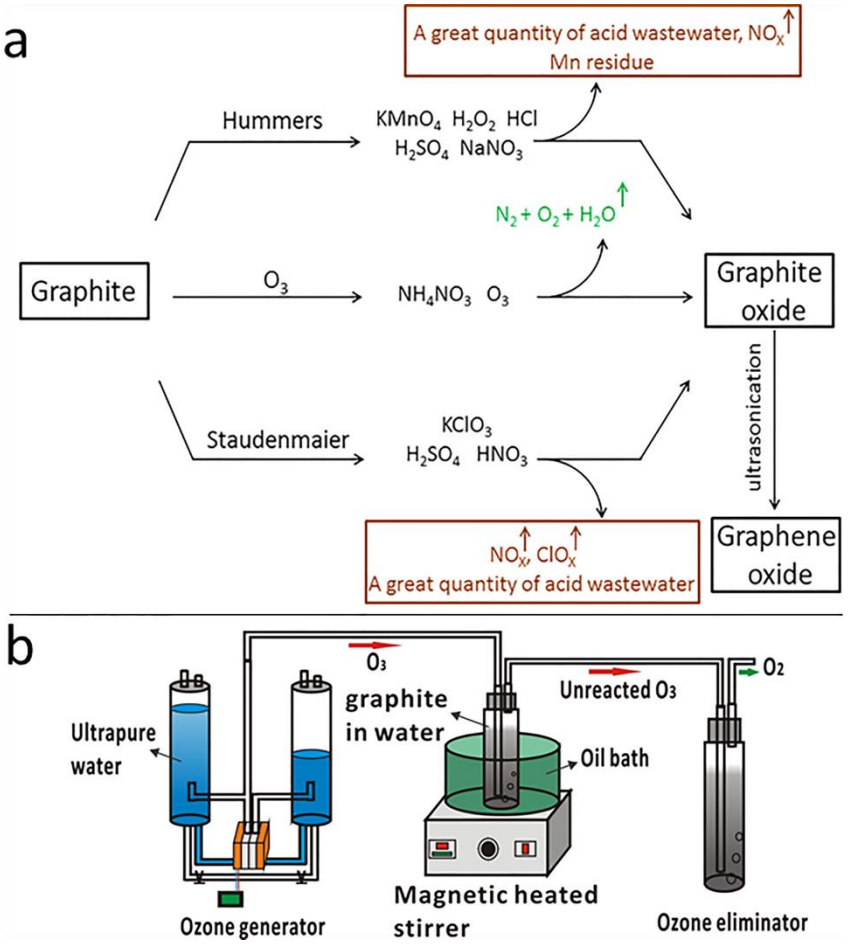

Fig. S1 (a) The contrast between representation of procedures of graphene oxide prepared by conventional methods and ozone oxidation. (b) Schematic illustration of ozonization process.

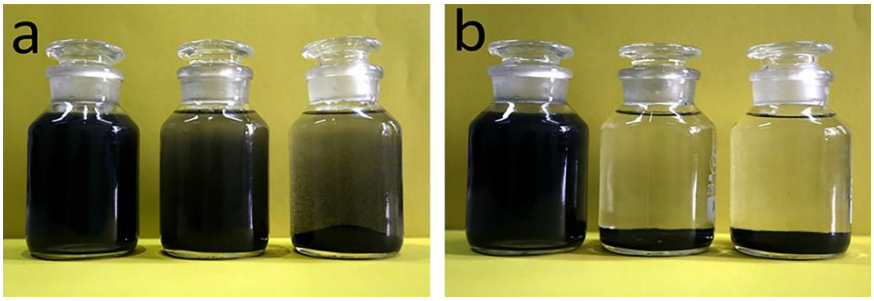

Fig. S2 Large scale graphene oxide, G-NH_4NO_3 and raw graphite dispersions in water respectively (from left to right). (a) Fifteen minutes later; (b) Five months later.

Fig. S2a shows the as-prepared large scale graphene oxide, G-NH_4NO_3 and raw graphite dispersions in water fifteen minutes later. We can see that the G-NH_4NO_3 and raw graphite gradually sank to the bottom of bottle in water. Fig. S2b shows graphene oxide, G-NH_4NO_3 and raw graphite dispersions in water for five months, respectively. The G-NH_4NO_3 and raw graphite settled completely in water, while graphene oxide solution was stable for five months or longer without any apparent aggregation due to the hydrophilic properties.

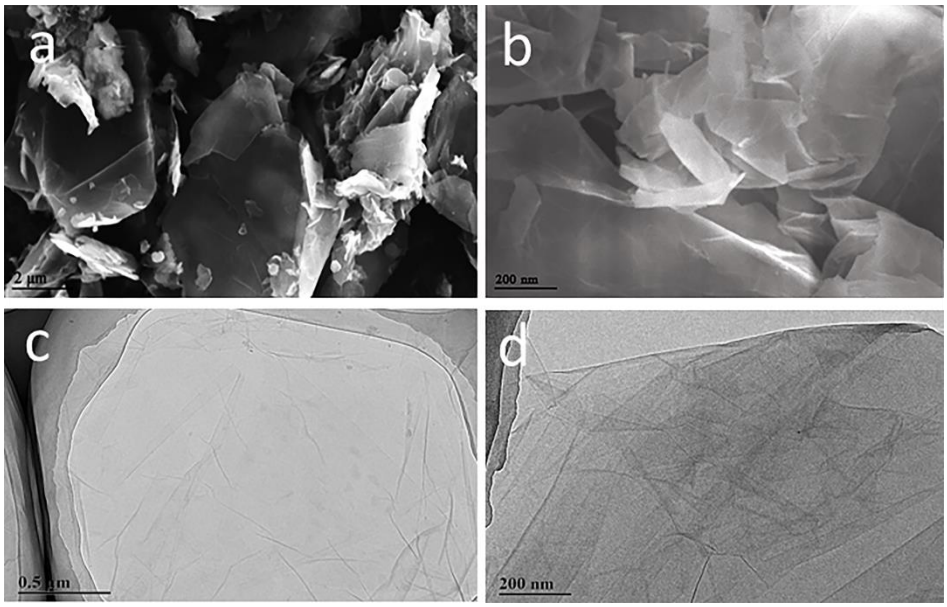

Fig. S3 (a) SEM image of pristine graphite. (b) SEM image of graphene oxide after oxidation of benzyl alcohol. (c) and (d) Bright-field TEM images of as-prepared GO (graphene oxide).

Fig. S3a shows the SEM image of pristine graphite, which appears as big blocks with obvious difference to graphene oxide. Fig. S3b demonstrates the SEM image of graphene oxide after the oxidation of benzyl alcohol. We can see that the graphene oxide flakes are also mostly wavy and wrinkled, maintaining its morphology before reaction. Fig. S3c and Fig. S3d show the bright-field TEM images of the exfoliated

GO typically observed. On the top of the grid, we can find that GO has a typical shape resembling the crumpled thin films, with a few hundred square nanometers. The films were close to semitransparent, scrolled, and slightly entangled with each other[1], revealing the disorder of the flakes.

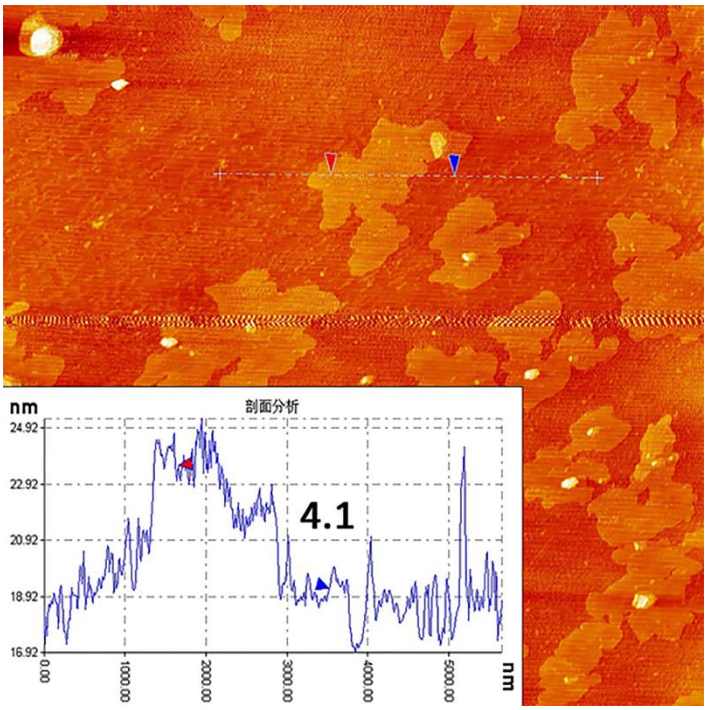

Fig. S4 AFM image of graphene oxide nanoplatelet. The inset shows the height profile through the line shown in Fig S4.

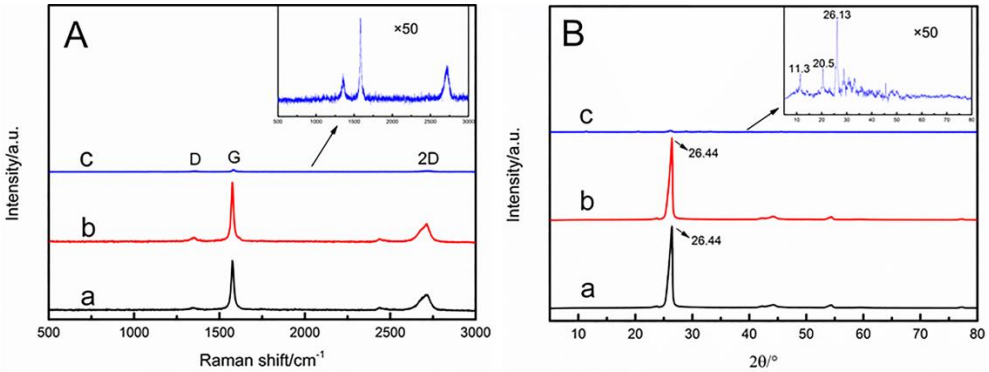

Fig. S5 (A) Raman spectra and (B) XRD patterns of graphite, G-NH_4NO_3, and as-prepared GO sample

Raman scattering, which is a noninvasive technique directly responded to the interactions between electron and phonon and is strongly sensitive to electronic properties[2], has been extensively applied to characterize the structure of graphite and

graphene materials. The Raman spectra of graphite (Fig. S5A-a), G-NH_4NO_3 (Fig. S5A-b), and GO sample (Fig. S5A-c) consist of the typical D-, G-, and 2D-bands of carbon. The inset is an enlarged view of GO. The D-band, at around 1350 cm^{-1}, is associated with the breathing mode of κ-point phonons of A_{1g} symmetry. The G-band, at around 1580 cm^{-1}, is due to the vibration of sp^2-bonded carbon atoms and corresponds to the E_{2g} phonon at the centre of Brillouin zone. The 2D-band is observed at around 2700 cm^{-1} and sometimes labeled as D´-band. The D and 2D bands are not used to determine the number of layers but to examine electronic effects[2]. After processing with NH_4NO_3 (Fig. S5A-b), the D mode slightly becomes stronger than graphite (Fig. S5A-a) by reason of a few defects increased during the thermal decomposition process of NH_4NO_3. After ozonization, the intensity of D-band increased obviously due to the charge transfer between ozone and graphite, implying a higher level of disorder degree of the GO layers and defects increased. In addition, I_D/I_G for GO sample increased markedly, suggesting an increase of the amount of carbon with sp^3 hybridization derived from sp^2 hybridization in the aromatic structure. Besides, the G-band position of GO sample shifts to higher position comparing to graphite and G-NH_4NO_3, which may attribute to the decreasing number of layers in their solid states.

The XRD spectrum of G-NH_4NO_3 (Fig. S5B-b) shows almost the same as that of raw graphite (Fig. S5B-a), the 002 peak at $2\theta=26.44°$ is the typical diffraction of graphite. However, the 002 peak is still presented in GO XRD spectrum (Fig. S5B-c) although it is very weak, which means that as-prepared GO (graphene oxide) may mix

with a small amount of graphite, and this coincides with the results of FT-IR analysis (Fig. 2b). On account of the formation of oxygen-containing functional groups on both sides of the graphene sheets and the occurance of sp^3 hybridization, such d-spacing is notably larger than that of single-layer raw graphene (～0.34 nm), and individual graphene oxide sheets is also thicker than individual raw graphene sheets. In addition, the peak at 2θ=20.5° was also monitored, we speculate that this peak is extremely likely to move to lower 2θ.

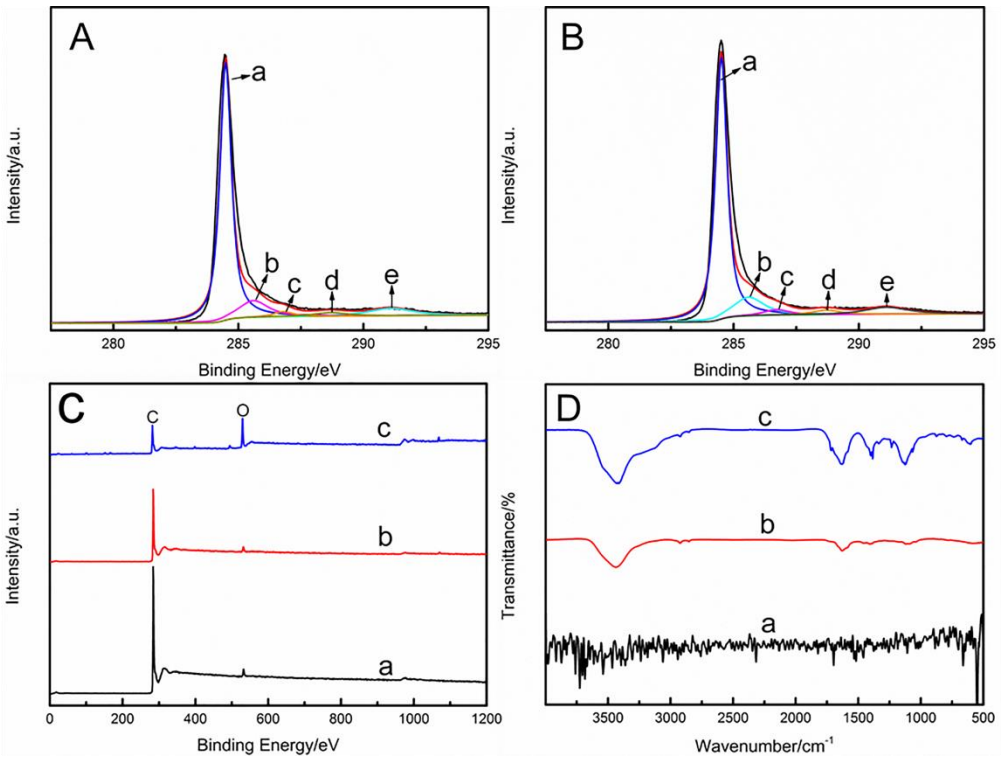

Fig. S6 (A) The C 1s XPS spectrum for graphite. (B) The C 1s XPS spectrum for G-NH_4NO_3. (C) XPS wide spectra of graphite, G-NH_4NO_3, and GO sample. (D) FT-IR spectra of graphite, G-NH_4NO_3, and GO sample.

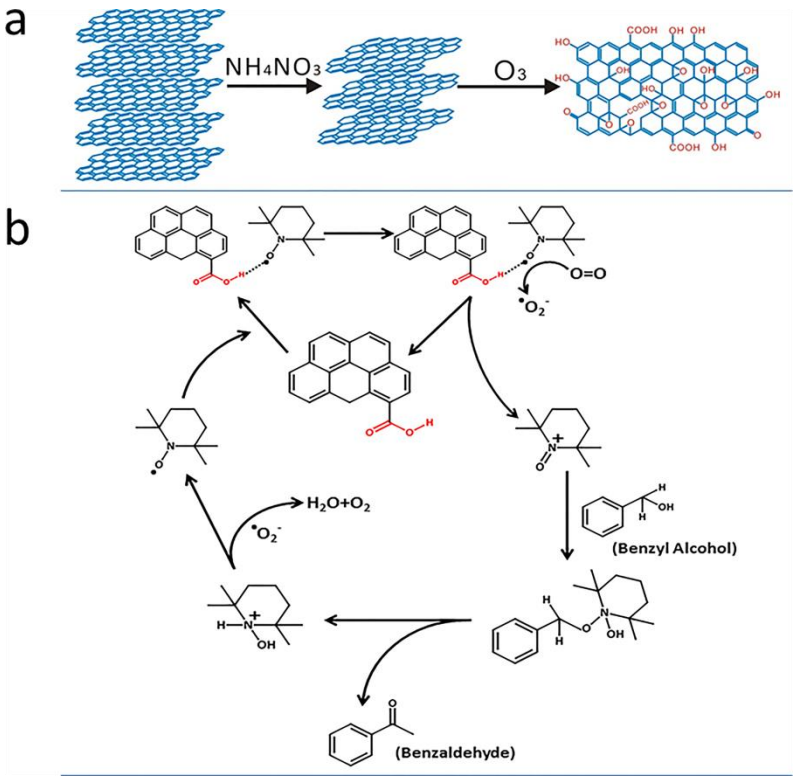

Fig. S7 (a) Proposed procedure of graphene oxide preparation. (b) Proposed reaction pathway for selective oxidation of benzyl alcohol to benzaldehyde with molecular oxygen as the terminal oxidant in the GO/TEMPO catalytic system.

It has been reported that the carboxyl groups in graphene oxide have oxidizing properties and there is linear relationship between oxidation ability and carboxyl group content[3]. The edge sites of GO, decorated with carboxyl groups and unpaired electrons, constitute the active sites and afford enhanced kinetics for the molecular TEMPO and oxygen trapping and activation by a sequence of electron transport[3, 4]. The content of carboxyl groups in our graphene oxide is very close to the graphene oxide prepared by Hummers method (Table S4), from which we can explain why there is just little difference in benzyl alcohol conversion rate in the presence of two kinds of graphene oxide. However, the decrease of benzaldehyde selectivity in the presence of graphene oxide prepared by Hummers method may be caused by the residual metal ions in the preparation process. One plausible mechanism showed in

Fig. S7b as the following: TEMPO binds to carboxyl groups via a hydrogen bond and forms an electron-donor complex. The molecular oxygen is reduced by the unpaired electrons in GO to form $\bullet O_2^-$. Simultaneously, the anchored TEMPO is oxidized by the positive charge in GO to form the oxoammonium cation and the active site on GO is regenerated. Benzyl alcohol was oxidized by the oxoammonium cation to benzaldehyde, with hydroxylamine producing. The hydroxylamine is reoxidized by $\bullet O_2^-$,and the TEMPO molecule is also regenerated. Sequentially, the by-product H_2O_2 decomposes into H_2O and O_2 under the reaction temperature[5]. The catalytic activity can further be improved through optimizing the reaction temperature and GO content. In a broader perspective, GO, used as a mental-free carbocatalyst, has the potential to facilitate synthetically useful transformations.

A plausible reaction pathway of GO (graphene oxide) preparation is proposed in Fig. S7a. The decomposition process of NH_4NO_3 at 390 ℃ immediately generated hot stream (N_2, O_2, H_2O), which can break large graphite blocks into smaller and thinner ones like explosives. The particle size distribution measured by Laser Particle analyzer gave the confirmation (Fig. 3d). When G-NH_4NO_3 was exposed to highly concentrated ozone, the edge and grain boundaries were oxidized due to the continuous attack from hydroxyl radicals (▪OH) result from the reaction of highly concentrated ozone and water[6]. The process of ozonization and ultrasonication slightly led to decrease in the size of graphene sheets (Fig. 3d). Based on the effect of NH_4NO_3 and highly concentrated ozone, we proposed the chemical structure of GO (Fig. S7a), where the oxygen-containing functional groups are believed to be

decorated mostly at the edges of a graphene plane.

Table S1 Comparison of oxidation ability of some oxidants (*calculation based on oxidation ability of Cl_2).

oxidant	oxidation potential (V)
F_2	3.06
▪ OH	2.80
O	2.42
O_3	2.07
Cl_2	1.36
H_2O_2	0.84
O_2	0.4

Table S2 XPS results: surface atomic composition for graphite, G-NH_4NO_3, and GO sample

Spectrum	Total content (%)		
	Graphite	G-NH_4NO_3	Graphene oxide
C 1s	97.06	96.74	64.66
O 1s	2.94	3.26	35.34
C : O	33.01 ： 1	29.67 ： 1	1.82 ： 1

Table S3 XPS results: surface atomic composition for graphite, G-NH_4NO_3, and GO sample

Spectrum	Singal	Graphite		G-NH_4NO_3		Graphene oxide	
		(eV)	(%)	(eV)	(%)	(eV)	(%)
C 1s	Peak a	284.5	73.04	284.5	71.26	284.8	27.29
	Peak b	285.6	11.56	285.6	12.99	285.5	22.24
	Peak c	286.8	2.30	286.7	3.17	286.7	7.57
	Peak d	288.7	2.87	288.7	2.99	289.4	7.56
	Peak e	291.1	7.28	291.1	6.33		

Table S4 XPS results: surface atomic composition for Graphene Oxide (Hummers) and Graphene Oxide (O_3).

	H-GO/%	O_3-GO/%
C=C	18.87	27.29
C=O	9.13	7.57
C-O	24.31	22.24
O-C=O	7.69	7.56
O	40.0	35.44

The X-ray photoelectron spectroscopy (XPS) is generally used to provide qualitative and quantitative information about chemical composition of sample

surface. Fig.S6A and Fig.S6B shows the C 1s XPS spectrum for graphite and G-NH_4NO_3, respectively. The C 1s XPS spectra includes five carbon species: (C-C) (peak a), carbon singly bounds to oxygen (C-O) (peak b), carbon doubly bounds to oxygen (C=O) (peak c), O-C=O (peak d), and carbon atoms assigned to π electrons within aromatic systems (peak e). For graphite, the amount of the surface hydroxyl group (peak b) is almost four times of the surface carboxyl group (peak d) (Table S3). After reaction with ozone, a considerable increase in hydroxyl group, simultaneously with a bit growth in carboxyl group (Table S3). In Fig. S6C, by comparing with the standard binding energy of elements, we can see that each of the three samples contain C, O elements. Then we quantitatively calculate C/O ratio of three samples, 33.01:1, 29.67:1, and 1.82:1, respectively (Table S2). Total amount of surface oxygen of G-NH_4NO_3, is a little higher than that in graphite, which is partially caused by the decomposition product (oxygen) of NH_4NO_3 within the layered structure of graphite[7]. Comparative analysis between graphite and graphene oxide reveals a remarkable increase of surface oxygen content after ozonization. Total content of surface oxygen in graphene oxide is almost twelve times (Table S2) than that in graphite, suggesting deep oxidation of graphite.

FT-IR is an essential tool to characterize chemical bonds or functional groups because of their different absorption frequencies in molecules. Fig. S6D shows FT-IR spectra of graphite, G-NH_4NO_3, and GO sample prepared after ozonization. Because raw graphite is too black to obtain available spectrum, we focus on relatively analyzing the other two spectra. In the spectrum of the G-NH_4NO_3 (Fig. S6D-b), the

broad, intense band at 3440 cm^{-1} can be attributed to O-H in water molecule stretching vibrations. The peak at 1385 cm^{-1} is from bending vibration of O-H in water molecule that comes out of water vapor in air and the peak at 1640 cm^{-1} is associated with stretching vibrations of C=C in graphite.

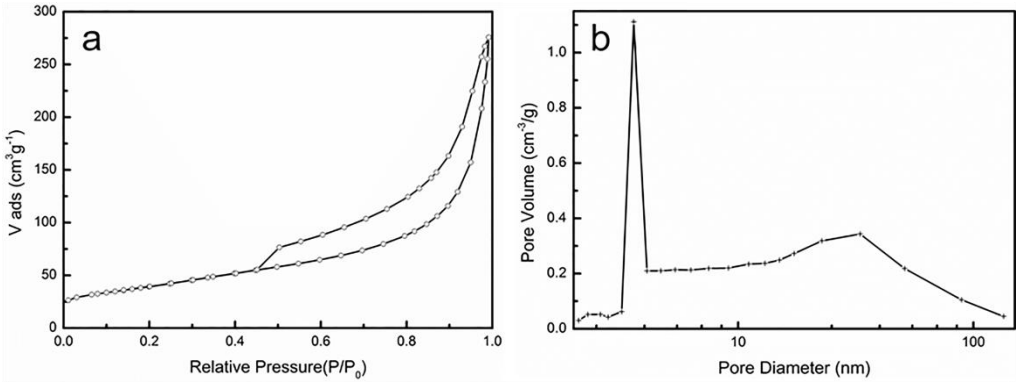

Fig. S8 (a) N_2 sorption of O_3-GO. (b) Pore size distribution of O_3-GO.

The specific surface area was determined by N_2 adsorption/desorption analysis and calculated by the Brunauer-Emmett-Teller (BET) model. The spectra of N_2 adsorption of O_3-GO is shown in Fig. S8 (a) and pore size distribution of O_3-GO in Fig. S8 (b). The O_3-GO has a BET surface area of 139.51 m^2/g with an average pore diameter of 12.23 nm.

References

1 M. Lotya, Y. Hernandez, P. J. King, R. J. Smith, V. Nicolosi, L. S. Karlsson, F. M. Blighe, S. De, Z. M. Wang, I. T. McGovern, G. S. Duesberg and J. N. Coleman, *J. Am. Chem. Soc.*, 2009, **131**, 3611-3620.

2 C. N. R. Rao, K. Biswas, K. S. Subrahmanyam and A. Govindaraj, *J. Mater. Chem.*, 2009, **19**, 2457-2469.

3 G. Lv, H. Wang, Y. Yang, T. Deng, C. Chen, Y. Zhu and X. Hou, *ACS. Catalysis.*, 2015, **5**, 5636-5646.

4 C. L. Su, M. Acik, K. Takai, J. Lu, S. J. Hao, Y. Zheng, P. P. Wu, Q. L. Bao, T. Enoki, Y. J. Chabal and K. P. Loh, *Nat. Commun.*, 2012, **3**, 1298.

5 A. Dijksman, A. Marino-Gonzalez, A. M. I. Payeras, I. W. C. E. Arends and R. A. Sheldon, *J. Am. Chem. Soc.*, 2001, **123**, 6826-6833.

6 K. C. Hwang and A. Sagadevan, *Science*, 2014, **346**, 1495-1498.

7 P. Krawczyk, *Chem. Eng. J.*, 2011, **172**, 1096-1102.